Plant Cell Rep (2017) 36:1917–1928
DOI 10.1007/s00299-017-2206-0

ORIGINAL ARTICLE

Endocytic pathways involved in PLGA nanoparticle uptake by grapevine cells and role of cell wall and membrane in size selection

Cleofe Palocci[1] · Alessio Valletta[2] · Laura Chronopoulou[1] · Livia Donati[2] · Marco Bramosanti[1] · Elisa Brasili[1] · Barbara Baldan[3] · Gabriella Pasqua[2]

Received: 6 July 2017 / Accepted: 5 September 2017 / Published online: 14 September 2017
© Springer-Verlag GmbH Germany 2017

Abstract

Key message **PLGA NPs' cell uptake involves different endocytic pathways. Clathrin-independent endocytosis is the main internalization route. The cell wall plays a more prominent role than the plasma membrane in NPs' size selection.**

Abstract In the last years, many studies on absorption and cell uptake of nanoparticles by plants have been conducted, but the understanding of the internalization mechanisms is still largely unknown. In this study, polydispersed and monodispersed poly(lactic-co-glycolic) acid nanoparticles (PLGA NPs) were synthesized, and a strategy combining the use of transmission electron microscopy (TEM), confocal analysis, fluorescently labeled PLGA NPs, a probe for endocytic vesicles (FM4-64), and endocytosis inhibitors (i.e., wortmannin, ikarugamycin, and salicylic acid) was employed to shed light on PLGA NP cell uptake in grapevine cultured cells and to assess the role of the cell wall and plasma membrane in size selection of PLGA NPs. The ability of PLGA NPs to cross the cell wall and membrane was confirmed by TEM and fluorescence microscopy. A strong adhesion of PLGA NPs to the outer side of the cell wall was observed, presumably due to electrostatic interactions. Confocal microscopy and treatment with endocytosis inhibitors suggested the involvement of both clathrin-dependent and clathrin-independent endocytosis in cell uptake of PLGA NPs and the latter appeared to be the main internalization pathway. Experiments on grapevine protoplasts revealed that the cell wall plays a more prominent role than the plasma membrane in size selection of PLGA NPs. While the cell wall prevents the uptake of PLGA NPs with diameters over 50 nm, the plasma membrane can be crossed by PLGA NPs with a diameter of 500–600 nm.

Keywords Microfluidics · Polymeric nanoparticles · Cell cultures · Endocytosis · *Vitis vinifera*

Abbreviations

PLGA NPs	Poly(lactic-co-glycolic) acid nanoparticles
TEM	Transmission electron microscope
FM4-64	*N*-(3-triethylammoniumpropyl) -4-(6-(4-(diethylamino) phenyl)hexatrienyl)pyridinium dibromide
ACN	Acetonitrile
HPLC	High-performance liquid chromatography
Cu6	Coumarin 6
CFM	Continuous flow microfluidic
OBM	Osmosis-based methodology
DLS	Dynamic light scattering
PdI	Polydispersity index
SEM	Scanning electron microscopy
DMSO	Dimethylsulfoxide
NAA	α-Naphthaleneacetic acid

Communicated by Kan Wang.

Electronic supplementary material The online version of this article (doi:10.1007/s00299-017-2206-0) contains supplementary material, which is available to authorized users.

✉ Alessio Valletta
alessio.valletta@uniroma1.it

[1] Department of Chemistry, University of Rome La Sapienza, Piazzale A. Moro 5, 00185 Rome, Italy

[2] Department of Environmental Biology, University of Rome La Sapienza, Piazzale A. Moro 5, 00185 Rome, Italy

[3] Department of Biology, University of Padua, Via Ugo Bassi 58/B, 35131 Padua, Italy

KIN Kinetin
PI3K Phosphatidylinositol 3-kinase

Background

In the last decades, many studies have been carried out on the ability of nanomaterials to interact with eukaryotic cells. Currently, this ability is mainly exploited for nanomedicine applications, to deliver bioactive molecules to animal cells (Couvreur 2013 and references cited therein Chronopoulou et al. 2015), and only recently researchers have begun to explore the potential of nanocarriers in the field of plant biology (Wang et al. 2016). In the near future, the development of nanoparticles (NPs) to use in agriculture and plant research will most likely allow several new applications, ranging from treatments with pesticides and fertilizers to the delivery of nucleic acids for genetic transformations (González-Melendi et al. 2008). The ability to specifically deliver selected bioactive molecules to plant cells could play an important role in developing new products and strategies for agro-food applications (Mura et al. 2013).

The cell uptake of NPs has been mainly studied in animal systems (for a review, see Kettler et al. 2014). Different endocytic pathways seem to be responsible for the internalization of NPs in animal cells, including phagocytosis, macropinocytosis, clathrin-mediated, and cavaeole-mediated endocytosis. However, these results cannot be used to model the internalization in plant cells, due to the presence of the cell wall, an additional barrier outside the plasma membrane.

Several mechanisms have been proposed for the uptake of NPs in plant cells (e.g., by binding to carrier proteins, through aquaporins, ion channels, creating new pores, or by binding to organic chemicals in the environmental media) (Rico et al. 2011). TEM analyses carried out on grapevine cells in our previous work (Valletta et al. 2014) suggest that poly(lactic-co-glycolic) acid nanoparticles (PLGA NPs) are internalized by endocytic vesicles.

Endocytosis in plants has been neglected until the early 2000s because of the erroneous belief that the turgor pressure generated by the vacuole could prevent the formation of endocytic vesicles (Aniento and Robinson 2005; Robinson et al. 2008). Endocytosis in plants has been definitively demonstrated using amphiphilic styryl dyes, primarily FM4-64, which inserts into the plasma membrane and then moves to the tonoplast (Bolte et al. 2004; Meckel et al. 2004).

As well known, in plant cells, endocytosis plays a crucial role in several vital processes, such as protein transport (Lam et al. 2005), membrane recycling (Geldner and Jurgens 2006), cell signaling (Holstein 2002), as well as internalization of cell wall (Šamaj et al. 2005) and external soluble components (Botha et al. 2008; Onelli et al. 2008). However, the vast majority of the studies performed to date have focused on clathrin-dependent endocytosis, and very limited evidence on clathrin-independent pathways is available (Moscatelli et al. 2007; Etxeberria et al. 2009; Sandvig et al. 2008; Bandmann and Homann 2012).

In particular, in the studies on endocytosis in plant cells, FM4-64 has often been used as a general endocytic tracer (Leborgne-Castel et al. 2008). Nevertheless, several authors have observed that this probe has a high specificity for the clathrin-coated vesicles (Dhonukshe et al. 2007; Pérez-Gómez and Moore 2007; Leborgne-Castel et al. 2008; Bandmann and Homann 2012), and it has consequently been used as a marker of clathrin-dependent endocytosis (Bandmann and Homann 2012). To the best of our knowledge, specific markers for non-clathrinic endocytic vesicles are not currently available. A strategy employed in a recent study makes use of the clathrin-dependent endocytosis inhibitors wortmannin and ikarugamycin for the monitoring of the non-clathrin uptake of fluorescent-labeled polystyrene nanobeads into tobacco BY2 cells (Bandmann and Homann 2012).

It has been shown that the ability of NPs to penetrate the plant cells and tissues depends on both the plant species and NP composition (Valletta et al. 2014 and literature therein cited). The cellular uptake also depends on NP size, in relation with the diameter of cell wall pores and endocytic vesicles. Several studies show that cell wall and plasma membrane are selective barriers that allow the entry into the plant cell only to NPs within a specific size range (for reviews, see Ma et al. 2010; Schwab et al. 2016; Tripathi et al. 2017). Bandmann and Homann (2012) demonstrated that the cell wall prevents the uptake of nanobeads with a diameter greater than 100 nm in BY-2 tobacco cells, while protoplasts (cells whose walls have been removed via enzymatic digestion) are able to internalize nanobeads with a diameter of up to 1000 nm. Serag et al. (2010) investigated the uptake of multiwalled carbon nanotubes (MWCNTs) in *Catharanthus roseus* protoplasts and observed that while MWCNTs with dimensions up to 600 nm could cross the plasma membrane, only MWCNTs smaller than 100 nm could enter plastids, vacuole, and nucleus. Studies like these point out the differences in the selectivity of cell wall and biological membranes. In a recent review, the size exclusion limits of barriers for the uptake and transport of NPs, resulting from the studies currently available, are reported (Wang et al. 2016). A deeper knowledge of these limits is of great interest, both for basic and applied research. Regarding the delivery of bioactive substances in plants, such knowledge would make it possible to design NPs according to the type of cargo and the cell target. NPs with dimensions below the

size exclusion limit imposed by cell wall and/or plasma membrane would be suitable for the delivery of molecules, such as elicitors, targeted to plant cells. Conversely, NPs with dimensions above the size exclusion limit would be preferable for substances, such as antimicrobial agents, that should be released outside plant cells.

In a previous work on grapevine cells (Valletta et al. 2014), we demonstrated the ability of PLGA NPs to penetrate into grapevine cells. In the present study, we employed microfluidic and bulk nanoprecipitation methodologies to fabricate fluorescent-labeled PLGA NPs in the size range from 30 nm to 1 μm. We investigated in depth the ability of PLGA NPs of different sizes to cross the cell wall and membrane. We conducted several uptake experiments on *Vitis vinifera* L. cv. Italia cultured cells, combining the use of transmission electron microscopy (TEM), confocal analysis, fluorescent PLGA NPs, a specific probe for endocytic vesicles (FM4-64), and endocytosis inhibitors (i.e., wortmannin, ikarugamycin and salicylic acid) to investigate the mechanism involved in cell internalization and to assess the role of plant cell wall and plasma membrane in the size selection of PLGA NPs.

Materials and methods

Materials

Poly(D,L)-lactic-co-glycolic acid (PLGA, lactide: glycolide 50:50, MW 50 kDa), acetonitrile (ACN) for HPLC, ultrapure water for HPLC, cellulose dialysis membranes (MW cutoff 14 kDa), coumarin 6 (Cu6) (98%), and all other chemicals were purchased from Sigma-Aldrich (Milan, Italy) and used as received. Zero-Dead Volume Valco Internal cross stainless steel Union bore, stainless steel capillary Tubings, and PEEK Tubings were purchased from Restek (Bellefonte, PA, USA) and used to assemble a microfluidic device, as reported previously (Bramosanti et al. 2017).

Synthesis of fluorescent PLGA NPs

For the preparation of empty and Cu6-loaded PLGA NPs (Cu6-PLGA NPs) smaller than 200 nm, we used a microfluidic approach. PLGA (1 mg mL^{-1}) and Cu6 (ratio 1/50 w:w) were dissolved in the ACN organic phase and injected in the microfluidic device (Fig. 1), in which water was chosen as the continuous phase. No precipitates were formed in the microchannels during flow-focusing experiments. The organic solvent was finally removed by evaporation under reduced pressure. Cu6-PLGA NPs and blank PLGA NPs bigger than 200 nm were prepared using a patented osmosis-based methodology (OBM)

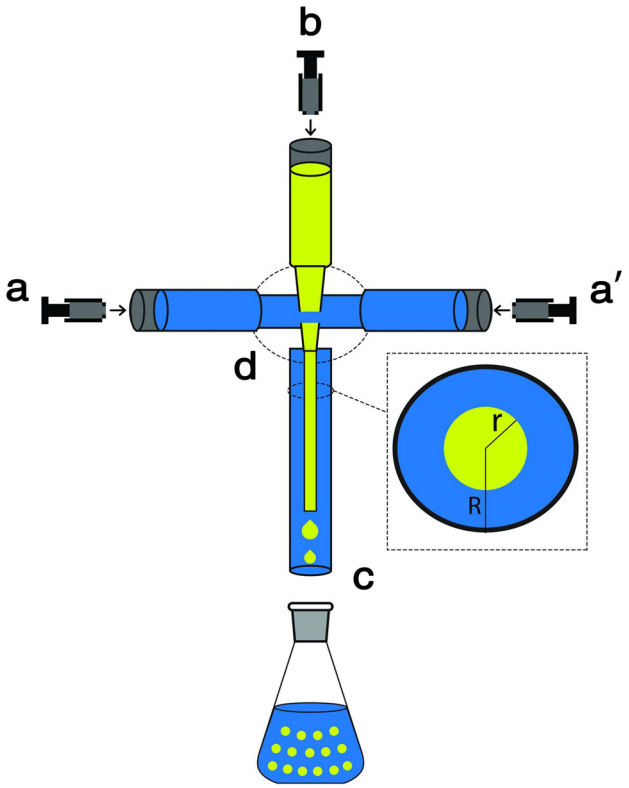

Fig. 1 Schematic diagram of the continuous flow microfluidic (CFM) reactor system used for the synthesis of PLGA NPs. The system consists of three inlets and one outlet (**c**) connected by a cross junction (**d**), creating a hydrodynamic flow-focusing with a central stream of dispersed phase (**b**) and two side streams of continuous phase (**a**, **a′**). The width of the focused central stream (R) can be varied by altering the volumetric flow rates of the three inlets or the internal dimensions of the mixing channel

(Chronopoulou et al. 2009). Briefly, PLGA (5 or 10 mg mL^{-1}) and Cu6 (ratio 1/50 w:w) were dissolved in DMSO. The obtained solution was transferred in a dialysis bag and immersed in H_2O. According to preliminary investigations, the osmotic equilibrium was reached after approximately 72 h. For both methodologies, the nanostructured polymer was recovered by centrifugation (14,000 rpm for 20 min), washed several times with non-solvent solution, centrifuged, and freeze-dried.

Chemico-physical characterization of PLGA NPs

Dynamic light scattering (DLS) using a Malvern Nano ZS instrument was employed to evaluate size, polydispersity index (PdI), and ζ-potential of the obtained NPs. Two mL of the produced PLGA NPs, suspensions were collected and used for microscopy analysis and size characterization. Measurements were performed in triplicate. Particle morphology was observed by scanning electron microscopy

(SEM) in both the secondary and the backscattered electron modes, using an LEO 1450VP SEM microscope.

Evaluation of Cu6 loading in PLGA NPs

Cu6 content of PLGA NPs was measured using a spectrophotometric method. Cu6-loaded PLGA NPs were dissolved in dimethylsulfoxide (DMSO), and then, the Cu6 content was determined by measuring the absorbance of the solution at $\lambda = 467$ nm and comparing it with a calibration curve.

Cell cultures and protoplast isolation

Cell suspension cultures of *V. vinifera* cv. Italia were obtained as reported by Santamaria et al. (2012) with slight modifications. Briefly, 3 g fresh weight (FW) of callus were inoculated in a 100 mL flasks containing 20 mL liquid B5 medium supplemented with 0.2 mg L^{-1} α-naphthaleneacetic acid (NAA), 1 mg L^{-1} kinetin (KIN), and 2% (w/v) sucrose, adjusted to pH 5.7 with NaOH 1 M. Subculturing was done every 20 days by transferring 3 g FW of suspended cells into 20 mL of fresh medium. Cell suspension cultures were maintained on a rotary shaker at 100 rpm under continuous darkness. Protoplasts were isolated as described by Fan et al. (2001) and stored in wash solution at 5 °C until use.

Endocytosis inhibitor treatment

Grapevine cells were inoculated in a sucrose-free culture medium (3 g FW in 20 mL). After 48 h of sucrose starvation, the cells were transferred in a fresh medium containing 2% (w/v) sucrose. The three specific endocytosis inhibitors wortmannin, ikarugamycin, and salicylic acid (all purchased from Sigma-Aldrich, Milan, Italy) were added to cell suspensions to a final concentration of 30, 10, and 100 μM, respectively. Cells were incubated with endocytosis inhibitors for 30, 60, 120, and 240 min, 480 min and 24 h before being subjected to microscopic analysis.

Administration of PLGA NPs

PLGA NPs were administered to cell cultures as reported by Valletta et al. (2014) with slight modifications. Briefly, freeze-dried Cu6-PLGA NPs were cold suspended by sonication in distilled water for 2 h. In all the experiments, Cu6-PLGA NPs were added to the liquid culture media at a final concentration of 15 mg L^{-1}. The observations were carried out 20-30 min after PLGA NPs' administration.

Fluorescence analysis

The localization of Cu6-PLGA NPs into *V. vinifera* suspended cells and protoplasts was visualized with an epifluorescence microscope apparatus described elsewhere (Valletta et al. 2014), fitted with a blue filter ($\lambda_{excitation}$ 386 nm; $\lambda_{emission}$ 490 nm). To label the plasma membrane and to monitoring the endocytic vesicle formation, cells and protoplasts were incubated at room temperature in 10 μM FM4-64 (Invitrogen, Dermstadt, Germany) for at least 10 min. Confocal analyses were carried out using a BD Carv II confocal microscope (BD Biosciences, San Jose, CA, USA) mounted on a Nikon Eclipse TE2000-U microscope with the MetaMorph 7.6 software (Universal Imaging, West Chester, PA). Excitation of FM4-64 was achieved with the 568 nm excitation line, with the resulting fluorescence observed using a 664–696 nm bandpass filter. Excitation of Cu6 was achieved with the 459 nm excitation line, with the resulting fluorescence observed using a 496–528 nm bandpass filter. Images were imported into BioImageXD 1.0 (r1799) (Kankaanpää et al. 2012) and fluorescent signals for FM4-64 and Cu6 thresholded. Subsequently, the amount of co-localization coefficients was calculated using the BioImageXD co-localization tool. Statistical significance of the results from four independent experiments was evaluated by paired Student's *t* test, considering significant difference with *P* values ≤ 0.05.

Transmission electron microscopy analysis

To confirm the involvement of endocytosis in cell uptake of PLGA NPs, to verify their accumulation into the cells, and to visualize their subcellular localization, *V. vinifera* cells were subjected to TEM analysis. Briefly, 20–30 min after the administration of monodisperse (30 nm Ø) or polydisperse (30–220 nm Ø) PLGA NPs, cells were collected by centrifugation ($100 \times g$ for 10 min at 4 °C) and fixed for 24 h in 0.1 M cacodylate buffer containing 3% glutaraldehyde at 4 °C. The cells were post-fixed with 1% of osmium tetroxide in 0.1 cacodylate buffer for 2 h at 4 °C, dehydrated through an ethanol series (25, 50, 75, and 100%), and then embedded in araldite resin. An ultramicrotome was used to prepare thin sections, which were stained with uranyl acetate and lead citrate and observed with an FEI TECNAI operating at 120 kV. For each sample, 30 micrographs coming from sections of three different resin blocks were examined.

Results and discussion

Synthesis of fluorescent PLGA NPs

The microfluidic reactor employed for NP preparation is an efficient and versatile reactor recently assembled in our laboratory. According to previously reported results (Bramosanti et al. 2017), by reducing the diameter of the mixing channel in which nanoprecipitation occurs and by modulating some physico-chemical parameters (i.e., flow of the dispersed and continuous phases), NP diameter can be modulated. Using this microfluidic approach, we prepared three sets of monodisperse NPs with the following sizes: 30, 80, and 150 nm (Table 1).

PLGA NPs were loaded with Cu6 to make them fluorescent. The amount of Cu6 entrapped within PLGA NPs was 20 μg mg^{-1}. The very low probe solubility in aqueous systems as well as the adsorption on PLGA NPs are responsible of the high amount of Cu6 entrapped within the polymeric matrix (almost 100%). SEM investigations showed a spherical morphology for PLGA NPs, as shown in Fig. 2.

DLS measurements carried out on PLGA NPs, synthesized with or without the fluorescent probe under the same experimental conditions, and showed that the presence of Cu6 did not modify significantly the dimensions and size distribution of NPs (see supplementary material Fig. S1). PLGA NPs obtained by OBM methodology (Chronopoulou et al. 2009) had a broad size distribution, as evidenced by DLS and SEM measurements (Fig. 2d).

To obtain materials with lower polydispersity and appropriate diameters, samples obtained with OBM methodology were filtered using nitrocellulose filters (0.8, 0.45, and 0.22 μm). PLGA NPs were recovered from the filter, washed, and redispersed in distilled water by sonication. This downstream procedure has allowed to obtain PLGA NPs with mean diameters of 300, 540, and 1000 nm (Table 2 and supplementary material Fig. S2). The ζ-potential for all samples fell within the range between −25 and −35 mV, indicating a good stability of the colloidal systems.

Internalization of PLGA NPs in *V. vinifera* cells and protoplasts

Cu6-PLGA NPs of different sizes were administered to grapevine cell suspension cultures. To stimulate endocytosis, the cells were previously subjected to a period of starvation and then supplied with sucrose. Cell starvation has been used in several studies to stimulate endocytosis in the plant cell (Yamada et al. 2005; Etxeberria et al. 2005).

In this study, grapevine cells were incubated with different suspensions of Cu6-PLGA NPs and then examined by fluorescence microscopy. The green Cu6 signal was observed only into the cells incubated with polydisperse suspension of Cu6-PLGA NPs with diameter ranging from 30 to 220 nm or with monodisperse suspensions of Cu6-PLGA NPs with a diameter of 30 nm. This results are in agreement with a previous study, in which we observed that only PLGA NPs with a diameter <50 nm are able to penetrate into grapevine cells (Valletta et al. 2014).

The ability of small PLGA NPs to cross the cell wall and membrane was confirmed by TEM analysis: administered NPs first sticked to the outer surface of the cell wall (Fig. 3a), before crossing the wall (Fig. 3b), localizing in the space between cell wall and plasma membrane (Fig. 3c), being then internalized by membrane vesicles (Fig. 3d). These observations suggest that internalized PLGA NPs are able to creep into the matrix spaces of the cell wall. The width of the cell wall pores has never been determined in grapevine cultured cells; however, in other plant species, their diameter appears to range between 5 and 20 nm (Fleischer et al. 1999; Nair et al. 2010). This observation suggests that the diameter of cell wall pores in grapevine cultured cells is greater than that observed in other species although of the same order of magnitude. This difference is not surprising, as the size dynamics of cell wall pores can vary depending on many factors, including the plant species, cell type, degree of development, and physiological state of the cell. Moreover, cell wall texture in cultured cells is less dense and less structurally organized, contributing to increase the space size in walls. In addition, it has been hypothesized that certain NPs may interact with the cell wall, inducing an enlargement of

Table 1 Operational parameters of CFM

NPs size (nm)	PdI (polydispersity Index)	Microchannel i.d. (mm)	Flow ratio $R = (\psi_{org}/\psi_{water})$	Mixing time (s) (Bramosanti et al. 2017)
30 ± 11	0.088	0.130	0.05	0.005
80 ± 32	0.102	0.254	0.05	0.021
150 ± 56	0.091	0.254	0.2	0.255

Mean diameters and PdI values of the obtained NPs. All data were calculated from the mean values obtained for at least three samples. The statistical error was reported as the standard deviation obtained from DLS measurements

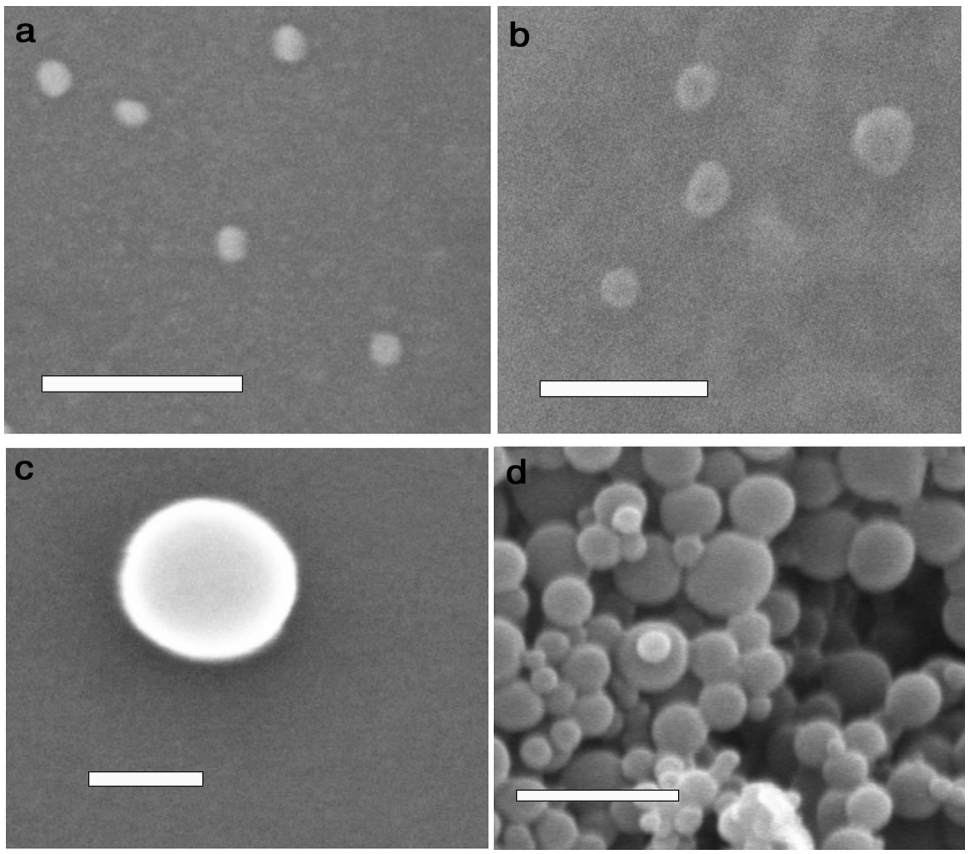

Fig. 2 SEM micrographs of Cu6-PLGA NPs prepared by the microfluidic flow-focusing methodology (**a**–**c**). **a** Capillary i.d. 0.130 mm, $R = 0.05$, scale bar = 200 nm; **b** capillary i.d. 0.254 mm, $R = 0.05$, scale bar = 300 nm; **c** capillary i.d. 0.254 mm, $R = 0.2$, scale bar = 100 nm; and **d** SEM micrograph of Cu6-PLGA NPs synthesized by OBM, scale bar = 2 μm

Table 2 Size and polydispersity of NPs obtained by OBM

NPs size (nm) (before filtration)	PdI (before filtration)	NPs size (nm) (after filtration)	PdI (after filtration)	PLGA Conc (mg mL^{-1})
372 ± 86	0.533	300 ± 53	0.113	5
418 ± 117	0.629	540 ± 72	0.096	5
841 ± 308	0.786	1000 ± 168	0.109	10

All data were calculated from the mean values obtained for at least three samples. The statistical error was reported as the standard deviation obtained from DLS measurements

the existing pores or the formation of new pores (Navarro et al. 2008; Ma et al. 2010).

In accordance with Bandmann and Homann (2012) and Valletta et al. (2014), in grapevine, cells PLGA NP-containing vesicles were observed exclusively in the cytoplasm. It was not possible to detect PLGA NPs inside the vacuole, neither with fluorescence microscopy nor with TEM and this suggests that NPs are not able to cross the tonoplast. Several studies have shown that the intracellular fate of NPs not only depends on the plant species, but also on the features of NPs, such as shape and size or chemical composition (Etxeberria et al. 2006; Liu et al. 2009; Ma et al. 2010; Bandmann and Homann 2012; Valletta et al. 2014). An individual plant cell may contain functionally distinct types of vacuoles, including lytic vacuoles that perform a general degradation function. In the perspective to use PLGA NPs as nanocarriers for the delivery of bioactive compounds in plants, it would be preferable if they were not directed to the lytic vacuole, where their cargo could be degraded before having exerted its biological activity.

In plant cells, the cargo internalized into the clathrin-coated vesicles is often destined to the lytic vacuole, via the *trans*-Golgi network, early endosomes and multivesicular bodies (daSilva et al. 2005; Robinson and Pimpl 2014; Fan et al. 2015). Probes such as FM4-64 are able to specifically label the clathrin-coated vesicles (Dhonukshe et al. 2007; Pérez-Gómez and Moore 2007; Leborgne-Castel et al. 2008; Bandmann and Homann 2012). By means of confocal microscopy, we have separately acquired the red fluorescence emitted by FM4-64 (corresponding to

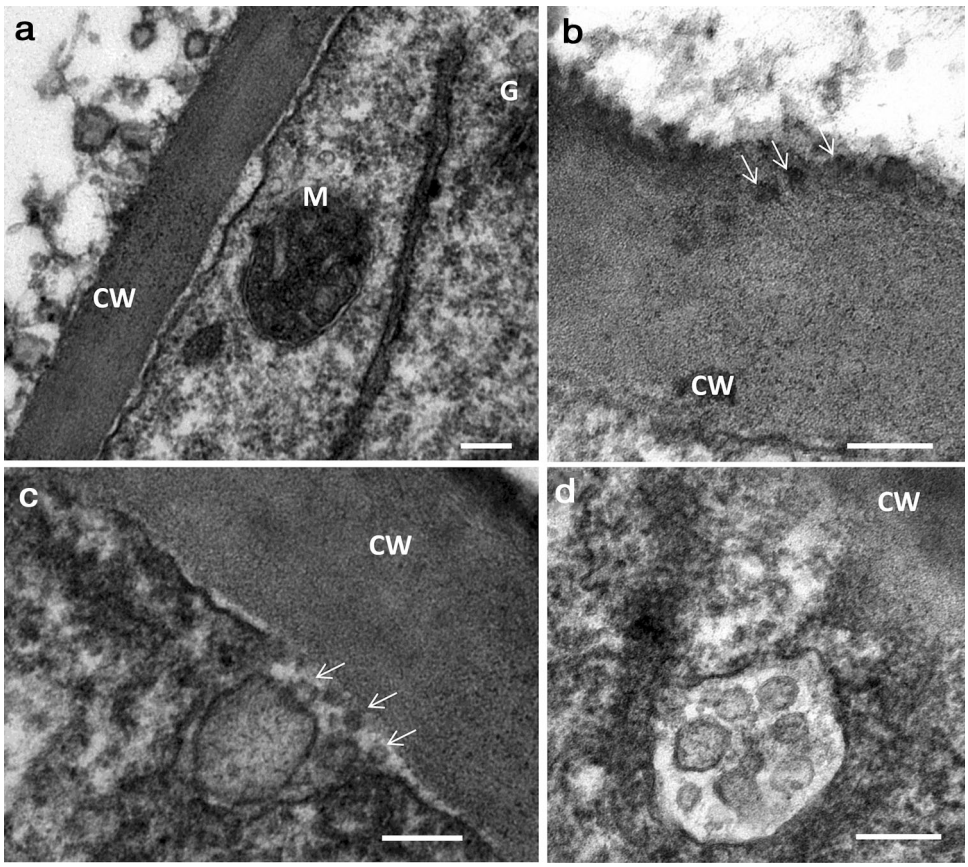

Fig. 3 TEM micrographs of grapevine cells incubated with a monodisperse PLGA NPs population (30–50 nm). **a** PLGA NPs adherent to the outer side of the cell wall; **b** PLGA NPs crossing the cell wall (white arrows); **c** PLGA NPs accumulated within the space between cell wall and plasma membrane; **d** an NP-containing vesicle. Scale bars in **a–c** represent 200 nm and in **d** 100 nm

clathrin-coated endocytic vesicles) and the green fluorescence emitted by Cu6 (corresponding to PLGA NP-containing vesicles) and we have evaluated the degree of co-localization (Fig. 4). In grapevine cells incubated with Cu6-PLGA NPs and simultaneously treated with FM4-64, vesicle bodies were frequently observed, in which the green and the red signals did not overlap. In these cells, it was recorded a highly variable co-localization rate from one cell to another, from 5 to 30% with a mean rate of 17% and a variance of 5.59×10^{-3}. This result suggests that PLGA NP uptake in grapevine cells largely follows the clathrin-independent endocytic route, and only secondarily the clathrin-dependent endocytic route. This agrees with the results obtained by Bandmann and Homann (2012) with polystyrene nanobeads and tobacco-cultured cells.

To further confirm the involvement of the clathrin-independent endocytic pathway in PLGA NP uptake, another set of experiments was carried out on grapevine in vitro-grown cells treated with the endocytosis inhibitors wortmannin, ikarugamycin, and salicylic acid. Wortmannin is a steroid compound of fungal origin, which has been widely used in plant cell biology to inhibit endocytosis. It is a very potent, specific, and irreversible phosphatidylinositol 3-kinase (PI3K) inhibitor in both animal and plant cells (Aniento and Robinson 2005). It has been recently demonstrated that wortmannin interfere with the distribution and dynamics of clathrin-coated pits on the plasma membrane (Ito et al. 2012 and literature therein cited), and consequently, it has been used as specific clathrin-dependent endocytosis inhibitor (Bandmann and Homann 2012). Ikarugamycin is an antibiotic isolated from *Streptomyces* sp., which has been shown to have antiprotozoal activity (Elkin et al. 2016). It is a selective, potent and acute inhibitor of clathrin-mediated endocytosis on plant cells (Moscatelli et al. 2007; Onelli et al. 2008; Elkin et al. 2016; Bandmann and Homann 2012). Salicylic acid is a phenolic compound involved in a broad range of biotic and abiotic stress responses, including immunity, defense-related cell death, and systemic acquired resistance (Vlot et al. 2009). Recently, it has observed that salicylic acid inhibits clathrin-mediated endocytosis in *Arabidopsis thaliana* (Du et al. 2013). The impact of this compound on clathrin-dependent endocytosis is not connected to the traditional signaling transduction pathway for transcription regulation, but instead involves its effect on the recruitment of clathrin on the plasma membrane: salicylic acid significantly reduces the incidence of clathrin light and heavy chain on the plasma membrane, suggesting that it affects endocytosis through clathrin (Du et al. 2013; Fan et al. 2015).

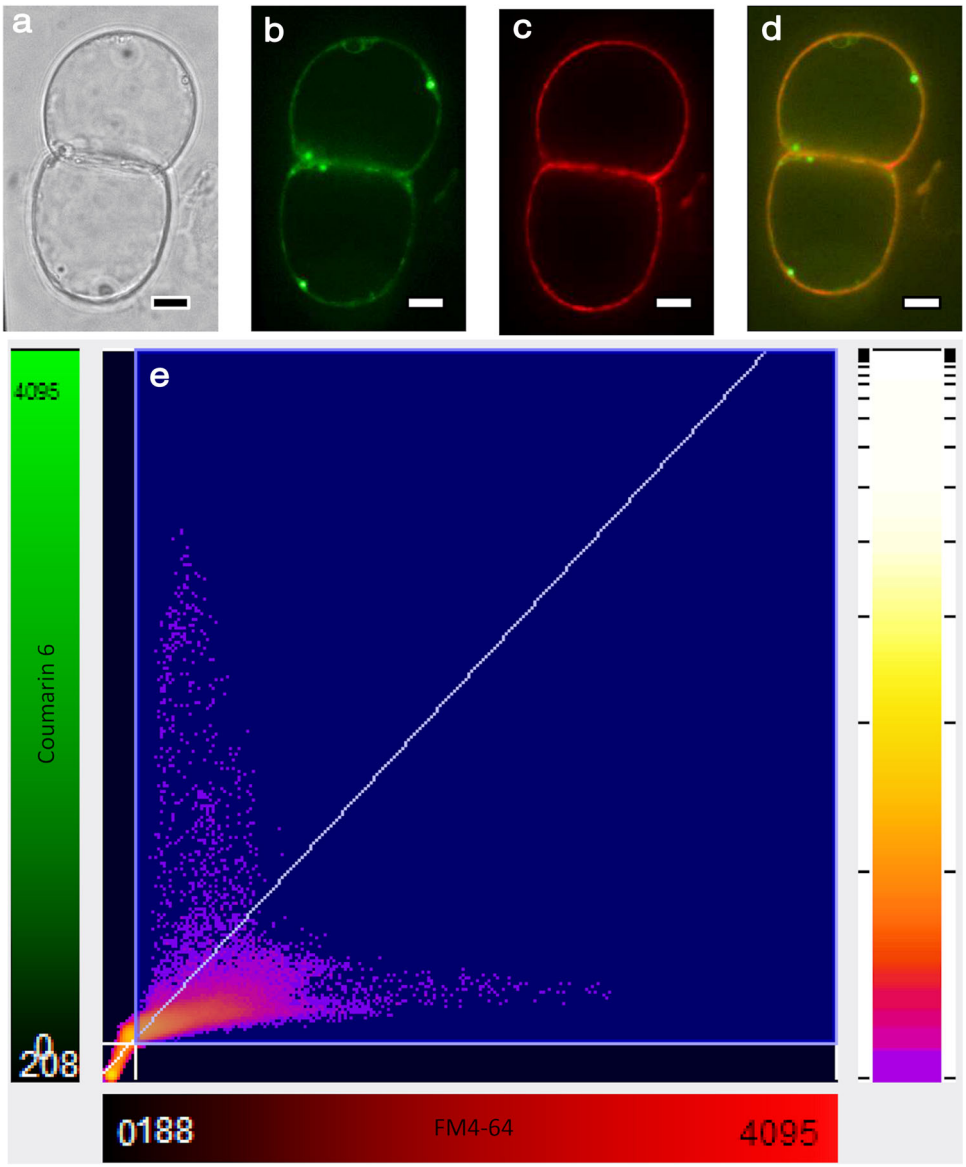

Fig. 4 Endocytic uptake of 30 nm Cu6-PLGA NPs into grapevine cells 20 min after the addition of PLGA NPs and FM4-64. Fluorescent images of grapevine cells observed in bright field (**a**) and under blue light (**b**–**d**), and quantitative analysis of co-localization of Cu6 (PLGANPs) and FM4-64 (clathrin-coated vesicles) as a scatter diagram (BioImageXD 1.0 software) (**e**). NPs accumulate in round spots in the cytosol (**b**) which partly co-localize with endocytic vesicles labeled by FM4-64 (**b**–**e**). All scale bars represent 20 µm

In the present study, grapevine cells pre-treated with such inhibitors for variable times, from 30 min to 24 h, were incubated with Cu6-PLGA NPs and then subjected to fluorescence analysis. None of the treatment suppressed the uptake of PLGA NPs. In Fig. 5, control cells are compared with the cells subjected to treatment with inhibitors for 60 min; similar fluorescence patterns were observed in cells treated for different times (data not shown). This observation represents a further evidence that clathrin-independent endocytic route is involved in PLGA NP cellular uptake in *V. vinifera* cells, as previously observed for polystyrene nanobead cellular uptake in BY-2 tobacco cells (Bandmann and Homann 2012).

In a previous study (Valletta et al. 2014), we observed that only PLGA NPs smaller than 50 nm were able to penetrate into grapevine cells. We hypothesized that the NP size-selection may be due to the cell wall. To verify this hypothesis, the FM4-64/Cu6 co-localization experiments were repeated on grapevine protoplasts incubated with monodispersed PLGA NPs of different sizes (Fig. 6). In the absence of the cell wall, PLGA NPs smaller than 540 nm could penetrate into the protoplasts. In the study by Bandmann and Homann (2012), tobacco protoplasts could internalize polystyrene nanobeads of higher sizes, up to 1000 nm. This could be explained with the different sizes of endocytic vesicles in different species or in different culture conditions. However, both studies indicate that the cell wall shows a higher selectivity than the cell membrane.

In the absence of the cell wall, PLGA NPs smaller than 540 nm were able to penetrate into the protoplasts. This clearly demonstrates that the cell wall is the main barrier

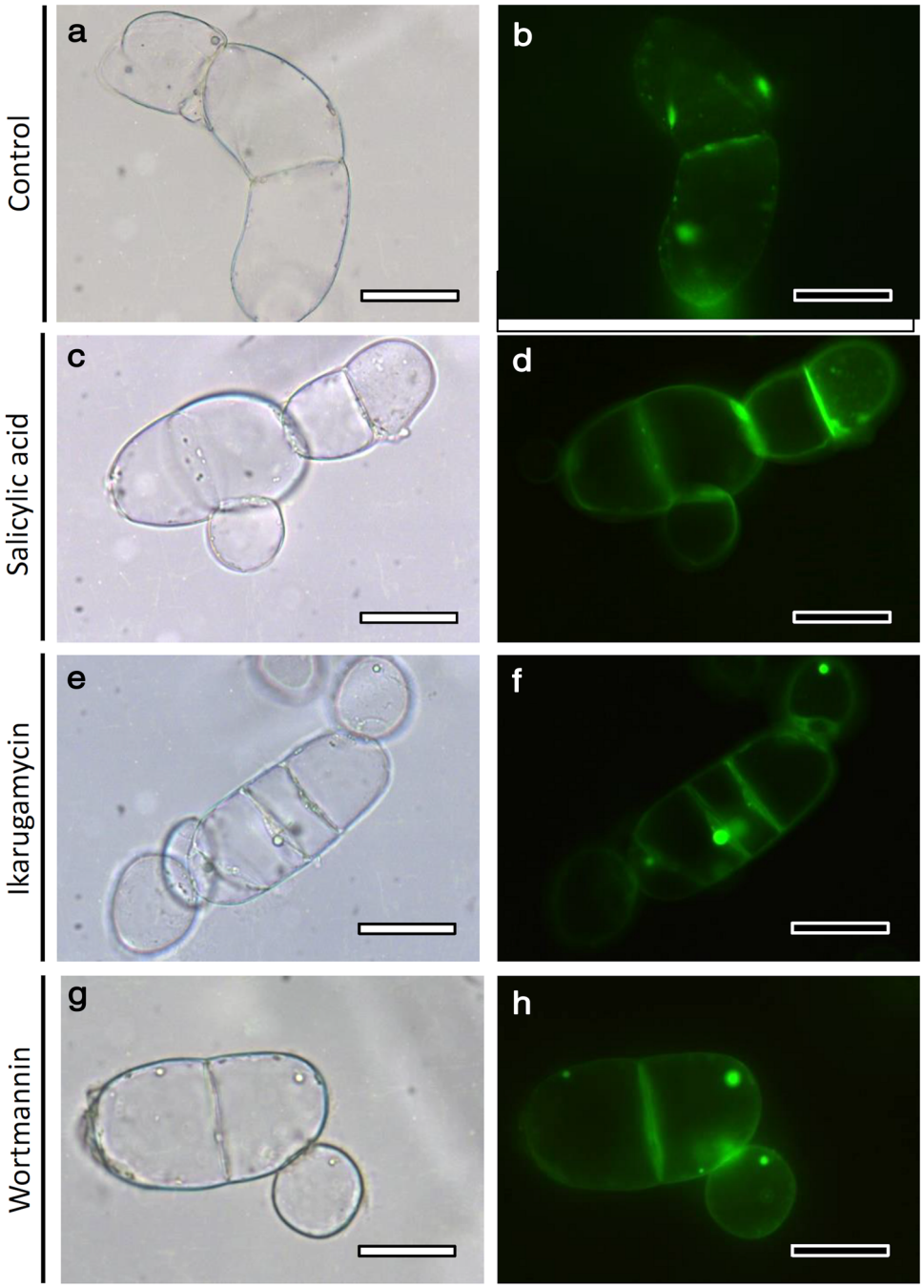

Fig. 5 Treatment for 60 min with three clathrin-dependent endocytosis inhibitors did not suppress the cellular uptake of Cu6-PLGA NPs. Control cells (**a**, **b**) and cells treated with 100 µM salicylic acid (**c**, **d**), 10 µM ikarugamycin (**e**, **f**), and 30 µM wortmannin (**g**, **h**). Cells observed under bright field (**a**, **c**, **e**, **g**) and under blue light (**b**, **d**, **f**, **h**). All scale bars represent 50 µm

that acts selectively on NP uptake as a function of particle dimensions.

Conclusions

In this study, we experimentally confirmed that the uptake of PLGA NPs in plant cells follows mainly the clathrin-independent endocytic pathway, suggesting that they are not directed to the lytic compartment. The absence of PLGA NPs into the vacuole was confirmed by fluorescence and electron microscopy. This finding is particularly interesting for the application of PLGA NPs as carriers for the delivery of bioactive compounds into the plants. Moreover, we highlighted the role of the cell wall and membrane in NP size selection. PLGA NPs which do not enter into the cell adhere quite strongly to the cell wall, probably because of attractive electrostatic interactions. The knowledge of this size exclusion limit exerted by the cell wall may allow to modulate NP uptake in agrochemical applications. In fact, NP penetration could be useful for the delivery of signaling molecules, including plant

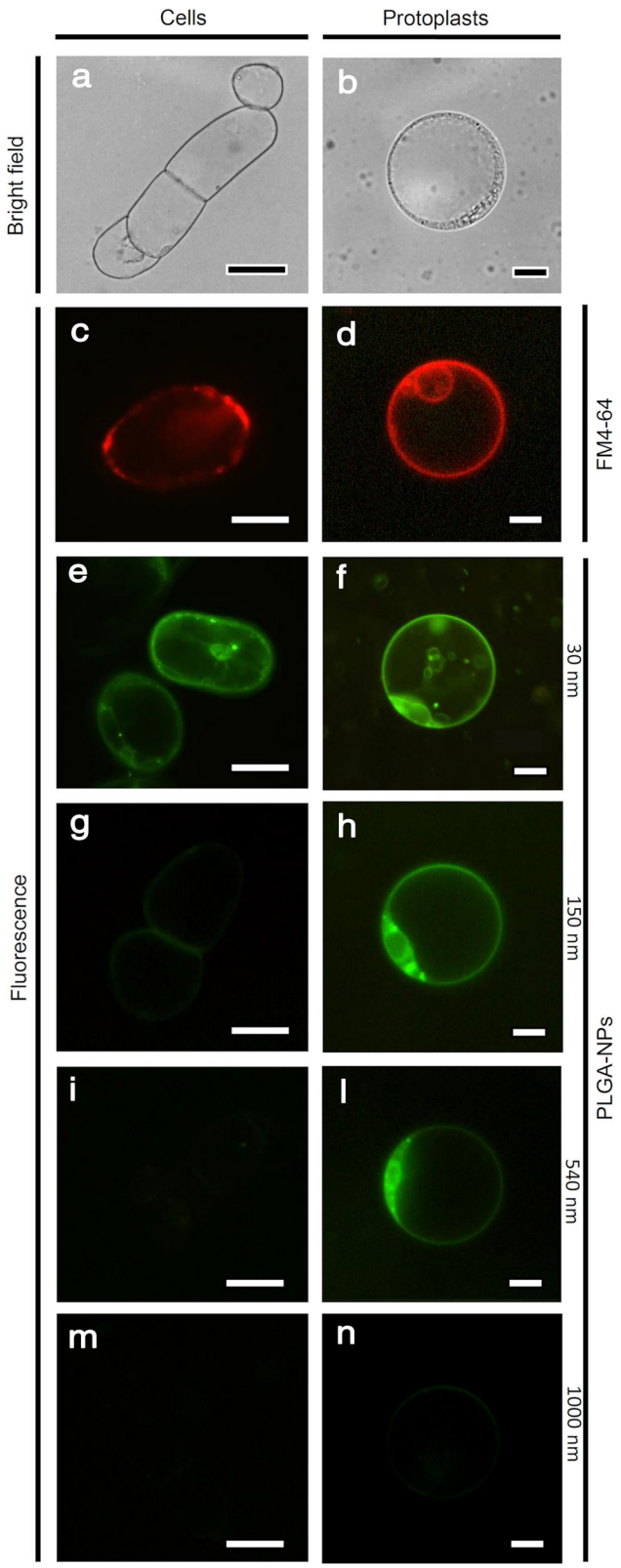

◀**Fig. 6** Cell wall and the cell membrane are involved in the selection of sizes of PLGA NPs which can penetrate into the cytoplasm. Grapevine cells (**a**) and protoplast (**b**) observed under bright field. The treatment with FM4-64 shows that clathrin-dependent endocytosis is active both in cells (**c**) and in protoplasts (**d**). PLGA NPs with diameter of 30 nm can penetrate the cells (**e**), while PLGA NPs bigger than 30 nm cannot cross the cell wall (**g**, **i**, **m**). PLGA NPs with diameter up to 540 nm can penetrate into the protoplasts (**f**, **h**, **l**), while PLGA NPs bigger than 540 nm cannot cross the cell membrane (**n**). All scale bars represent 20 μm

hormones, growth factors, and elicitors. Conversely, NP permanence on the outer side of the cell wall would be preferable for the delivery of drugs against pests and herbivores.

Author contribution statement MB synthesized and characterized NPs; AV and LD performed cell experiments and fluorescence analysis; BB performed TEM analysis; AV, LD, MB, LC, EB, and CP analyzed data; AV, LD, MB, LC, and CP wrote the manuscript; AV, CP, and GP and conceived the study; and GP supervised the research project.

Acknowledgements This study was supported by the University of Rome La Sapienza, Grant No. C26A13L5HT. The authors wish to thank the Electron Microscopy Service (Department of Biology, University of Padova, Italy) for providing technical support in TEM observations.

Compliance with ethical standards

Conflict of interest The authors declare that they have no conflict of interest.

References

Aniento F, Robinson DG (2005) Testing for endocytosis in plants. Protoplasma 226:3–11

Bandmann V, Homann U (2012) Clathrin-independent endocytosis contributes to uptake of glucose into BY-2 protoplasts. Plant J 70:578–584

Bolte S, Talbot C, Boutte Y, Catrice O, Read ND, Satiat-Jeunemaitre B (2004) FM-dyes as experimental probes for dissecting vesicle trafficking in living plant cells. J Microsc 214:159–173

Botha CE, Aoki N, Scofield GN, Liu L, Furbank TR, White RG (2008) A xylem sap retrieval pathway in ricer leaf blades: evidence of a role for endocytosis. J Exp Bot 59:2945–2954

Bramosanti M, Chronopoulou L, Grillo F, Valletta A, Palocci C (2017) Microfluidic-assisted nanoprecipitation of antiviral-loaded polymeric nanoparticles. Col Surf A. doi:10.1016/j.colsurfa.2017.04.062 **(in press)**

Chronopoulou L, Fratoddi I, Palocci C, Venditti I, Russo MV (2009) Osmosis based method drives the self-assembly of polymeric chains into micro- and nanostructures. Langmuir 25:11940–11946

Chronopoulou L, Nocca G, Amalfitano A, Callà C, Arcovito A, Palocci C (2015) Dexamethasone-loaded biopolymeric

nanoparticles promote gingival fibroblasts differentiation. Biotechnol Progr 3:1381–1387
Couvreur P (2013) Nanoparticles in drug delivery: past, present and future. Adv Drug Deliv Rev 65:21–23
daSilva LL, Taylor JP, Hadlington JL, Hanton SL, Snowden CJ, Fox SJ, Foresti O, Brandizzi F, Denecke J (2005) Receptor salvage from the prevacuolar compartment is essential for efficient vacuolar protein targeting. Plant Cell 17:132–148
Dhonukshe P, Aniento F, Hwang I, Robinson DG, Mravec J, Stierhof YD, Friml J (2007) Clathrin-mediated constitutive endocytosis of PIN auxin efflux carriers in *Arabidopsis*. Curr Biol 17:520–527
Du Y, Tejos R, Beck M, Himschoot E, Li H, Robatzek S, Vanneste S, Friml J (2013) Salicylic acid interferes with clathrin-mediated endocytic protein trafficking. Proc Natl Acad Sci 110:7946–7951
Elkin SR, Oswald NW, Reed DK, Mettlen M, MacMillan JB, Schmid SL (2016) Ikarugamycin: a natural product inhibitor of clathrin-mediated endocytosis. Traffic 17:1139–1149
Etxeberria E, Baroja-Fernandez E, Muñoz FJ, Pozueta-Romero J (2005) Sucrose-inducible endocytosis as a mechanism for nutrient uptake in heterotrophic plant cells. Plant and Cell Physiol 46:474–481
Etxeberria E, Gonzalez P, Baroja-Fernandez E, Romero JP (2006) Fluid phase endocytic uptake of artificial nano-spheres and fluorescent quantum dots by sycamore cultured cells: evidence for the distribution of solutes to different intracellular compartments. Plant Signal Behav 1:196–200
Etxeberria E, Gonzalez P, Pozueta J (2009) Evidence for two endocytic transport pathways in plant cells. Plant Sci 177:341–348
Fan LM, Wang YF, Wang H, Wu WH (2001) In vitro *Arabidopsis* pollen germination and characterization of the inward potassium currents in *Arabidopsis* pollen grain protoplasts. J Exp Bot 52:1603–1614
Fan L, Li R, Pan J, Ding Z, Lin J (2015) Endocytosis and its regulation in plants. Trends Plant Sci 20:388–397
Fleischer A, O'Neill MA, Ehwald R (1999) The pore size of non-graminaceous plant cell walls is rapidly decreased by borate ester cross-linking of the pectic polysaccharide rhamnogalacturonan II. Plant Physiol 121:829–838
Geldner N, Jurgens G (2006) Endocytosis in signaling and transport. Curr Opin Plant Biol 9:589–594
González-Melendi P, Fernández-Pacheco R, Coronado MJ, Corredor E, Testillano PS, Risueño MC, Ibarra MR, Rubiales B, Pérez-de-Luque A (2008) Nanoparticles as smart treatment-delivery systems in plants: assessment of different techniques of microscopy for their visualization in plant tissues. Ann Bot 101:187–195
Holstein SE (2002) Clathrin and plant endocytosis. Traffic 3:614–620
Ito E, Fujimoto M, Ebine K, Uemura T, Ueda T, Nakano A (2012) Dynamic behavior of clathrin in *Arabidopsis thaliana* unveiled by live imaging. Plant J 69:204–216
Kankaanpää P, Paavolainen L, Tiitta S, Karjalainen M, Päivärinne J, Nieminen J, Marjomäki V, Heino J, White DJ (2012) BioImageXD: an open, general-purpose and high-throughput image-processing platform. Nat Methods 9:683–689
Kettler K, Veltman K, van de Meent D, van Wezel A, Hendriks AJ (2014) Cellular uptake of nanoparticles as determined by particle properties, experimental conditions, and cell type. Environ Toxicol Chem 33:481–492
Lam SK, Tse YC, Jiang L, Oliviusson P, Heinzerling O, Robinson DG (2005) Plant prevacuolar compartment and endocytosis. Plant Cell Monogr 1:37–61
Leborgne-Castel N, Lherminier J, Der C, Fromentin J, Houot V, Simon-Plas F (2008) The plant defense elicitor cryptogein stimulates clathrin-mediated endocytosis correlated with reactive oxygen species production in bright yellow-2 tobacco cells. Plant Physiol 146:1255–1266
Liu Q, Chen B, Wang Q, Shi X, Xiao Z, Lin J, Fang X (2009) Carbon nanotubes as molecular transporters for walled plant cells. Nano Lett 9:1007–1010
Ma X, Geiser-Lee J, Deng Y, Kolmakov A (2010) Interactions between engineered nanoparticles (ENPs) and plants: phytotoxicity, uptake and accumulation. Sci Total Environ 408:3053–3061
Meckel T, Hurst AC, Thiel G, Homann U (2004) Endocytosis against high turgor: intact guard cells of *Vicia faba* constitutively endocytose fluorescently labeled plasma membrane and GFP-tagged K-channel KAT1. Plant J 39:182–193
Moscatelli A, Ciampolini F, Rodighiero S, Onelli E, Cresti M, Santo N, Idilli A (2007) Distinct endocytic pathways identified in tobacco pollen tubes using charged nanogold. J Cell Sci 120:3804–3819
Mura S, Seddaiu G, Bacchini F, Roggero PP, Greppi GF (2013) Advances of nanotechnology in agro-environmental studies. Ital J Agron 8:18
Nair R, Varghese SH, Nair BG, Maekawa T, Yoshida Y, Kumar DS (2010) Nanoparticulate material delivery to plants. Plant Sci 179:154–163
Navarro E, Baun A, Behra R, Hartmann NB, Filser J, Miao AJ, Sigg L (2008) Environmental behavior and ecotoxicity of engineered nanoparticles to algae, plants, and fungi. Ecotoxicol 17:372–386
Onelli E, Prescianotto-Baschong C, Caccianiga M, Moscatelli A (2008) Clathrin-dependent and independent endocytic pathways in tobacco protoplasts revealed by labeling with charged nanogold. J Exp Bot 59:3051–3068
Pérez-Gómez J, Moore I (2007) Plant endocytosis: it is clathrin after all. Curr Biol 17:R217–R219
Rico CM, Majumdar S, Duarte-Gardea M, Peralta-Videa JR, Gardea-Torresdey JL (2011) Interaction of nanoparticles with edible plants and their possible implications in the food chain. J Agric Food Chem 59:3485–3498
Robinson DG, Pimpl P (2014) Clathrin and post-golgi trafficking: a very complicated issue. Trends Plant Sci 19:134–139
Robinson DG, Jiang L, Schumacher K (2008) The endosomal system of plants: charting new and familiar territories. Plant Physiol 147:1482–1492
Šamaj J, Read ND, Volkmann D, Menzel D, Baluška F (2005) The endocytic network in plants. Trends Cell Biol 15:425–433
Sandvig K, Torgersen ML, Raa HA, Van Deurs B (2008) Clathrin-independent endocytosis: from nonexisting to an extreme degree of complexity. Histochem Cell Biol 129:267–276
Santamaria AR, Innocenti M, Mulinacci N, Melani F, Valletta A, Sciandra I, Pasqua G (2012) Enhancement of viniferin production in *Vitis vinifera* L. cv. Alphonse Lavallée Cell suspensions by low-energy ultrasound alone and in combination with methyl jasmonate. J Agric Food Chem 60:11135–11142
Schwab F, Zhai G, Kern M, Turner A, Schnoor JL, Wiesner MR (2016) Barriers, pathways and processes for uptake, translocation and accumulation of nanomaterials in plants—critical review. Nanotoxicology 10:257–278
Serag MF, Kaji N, Gaillard C, Okamoto Y, Terasaka K, Jabasini M, Tokeshi M, Mizukami H, Bianco A, Baba Y (2010) Trafficking and subcellular localization of multiwalled carbon nanotubes in plant cells. ACS Nano 5:493–499
Tripathi DK, Singh S, Singh S, Pandey R, Singh VP, Sharma NC, Prasad SM, Dubey NK, Chauhan DK (2017) An overview on manufactured nanoparticles in plants: uptake, translocation, accumulation and phytotoxicity. Plant Physiol Biochem 110:2–12
Valletta A, Chronopoulou L, Palocci C, Baldan B, Donati L, Pasqua G (2014) Poly(lactic-co-glycolic) acid nanoparticles uptake by

Vitis vinifera and grapevine-pathogenic fungi. J Nanopart Res 16:2744

Vlot AC, Dempsey DMA, Klessig DF (2009) Salicylic acid, a multifaceted hormone to combat disease. Ann Rev Phytopathol 47:177–206

Wang P, Lombi E, Zhao FJ, Kopittke PM (2016) Nanotechnology: a new opportunity in plant sciences. Trends Plant Sci 21:699–712

Yamada K, Fuji K, Shimada T, Nishimura M, Hara-Nishimura I (2005) Endosomal proteases facilitate the fusion of endosomes with vacuoles at the final step of the endocytotic pathway. Plant J 41:888–898